Noname manuscript No.
(will be inserted by the editor)

P2 - A new measurement of the weak charge of the proton

D. Becker · S. Baunack · F. E. Maas

Received: date / Accepted: date

Abstract After ten years of experience with parity-violating electron-proton-scattering, the preparatory work on a new high precision parity-violation experiment in Mainz has begun. Project P2 is bound to measure the weak charge of the proton to a relative uncertainty of 1.9 %, which corresponds to a relative uncertainty of 0.15 % for $\sin^2\theta_W$.
This can be achieved by measuring the parity-violating asymmetry in elastic electron-proton-scattering to a relative precision of 1.7 % at $E_{beam} \sim 200$ MeV and $Q^2 \sim 0.005$ GeV^2.
In this proceeding, we will discuss the achievable precision within project P2 as well as the experimental concept and present first results of studies involving Monte Carlo methods.

1 Introduction

The proton's weak charge at tree level is given by

$$Q_W^p = 1 - 4\sin^2\theta_W, \tag{1}$$

where θ_W is the electroweak mixing angle. In the Standard Model, relations between boson masses and coupling constants can be expressed in terms of θ_W. Therefore $\sin^2\theta_W$ can be considered the most central parameter in the theory of electroweak interactions.
Renormalization causes $\sin^2(\theta_W)$ to run as a function of the energy scale μ,

D. Becker
Institute of Nuclear Physics,
Johannes Gutenberg University Mainz,
Johann-Joachim-Becher-Weg 45,
D 55128 Mainz
Tel.: +49 6131-39-25369
E-mail: beckerd@kph.uni-mainz.de

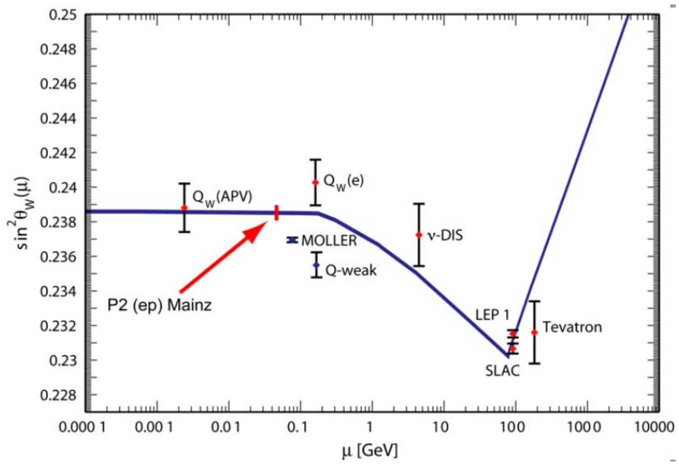

Fig. 1 Energy dependency of the electroweak mixing angle [1]. The blue line is the Standard Model prediction for the running of $\sin^2\theta_W$. Also included are results from recent measurements as well as projections of future results (QWeak [2], Møller [3], P2).

which can be identified with the momentum transfer Q. Fig. 1 shows the running of $\sin^2\theta_W(\mu)$ together with results of already performed and planned experiments.

Precise determinations of the weak mixing angle allow for a stringent test of the Standard Model, but one can also gain sensitivity to new physics in case of results differing from Standard Model predictions. Through complementary

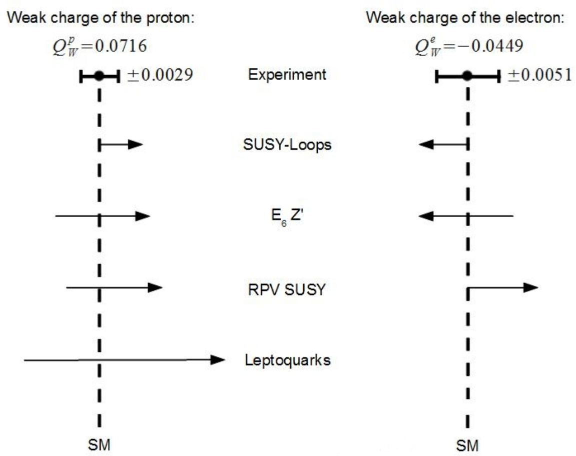

Fig. 2 Model-dependent shift predictions of the electron's and proton's weak charges Q_W^e and Q_W^p [4]. On top are the Standard Model predictions for the charges' values. The arrows indicate the shifts predicted by the different models. Depending on the model, the predictions differ in direction and size. In this manner, complementary measurements of the weak charges can give important hints at possibly correct extensions of the Standard Model.

measurements of the weak charges of both electron and proton, it is possible to narrow down possible extensions of the Standard Model. Fig. 2 illustrates how this can be achieved.
P2 aims at a determination of the proton's weak charge to a relative uncertainty of 1.9 % at the MAMI accelerator facility in Mainz. The following sections will give a brief overview on the planned experiment.

2 Experimental access to the weak charge of the proton

P2's experimental observable is the parity-violating asymmetry A_{PV} in elastic electron-proton-scattering at low momentum transfer. Fig 3 illustrates the measurement principle.
A_{PV} is an asymmetry in the cross section $\sigma^{\pm}$ of longitudinally polarized electrons with helicities $h = +1$ and $h = -1$ scattered off protons:

$$A_{PV} \equiv \frac{\sigma^+ - \sigma^-}{\sigma^+ + \sigma^-} = \frac{-G_F Q^2}{4\sqrt{2}\pi\alpha} \left(Q_W^p - F(Q^2)\right), \tag{2}$$

where G_F is Fermi's coupling constant, Q is the negative four-momentum-transfer, α is the electromagnetic coupling constant, Q_W^p the weak charge of the proton and

$$F(Q^2) = F_{em}(Q^2) + F_{axial}(Q^2) + F_{strange}(Q^2) \tag{3}$$

gives the hadronic contributions due to the proton's electromagnetic, axial and strange form factors.
At low Q^2, A_{PV} is dominated by the contribution from the proton's weak charge, as Fig. 4 shows for the projected conditions at the P2 experiment.
Therefore a measurement of A_{PV} at low momentum transfer gives access to the weak charge of the proton.
Since the statistical uncertainty is

$$\Delta A_{PV}^{stat} \approx \frac{1}{\sqrt{N}}, \tag{4}$$

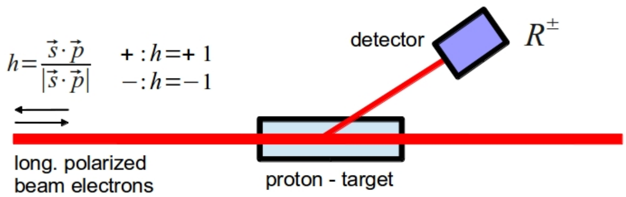

Fig. 3 Schematic sktech of P2's measurement principle: Longitudinally polarized beam electrons with helicity $h = +1$ or $h = -1$ hit a proton target and are detected after scattering. In case of elastic scattering, the main contribution to the cross section depends on the lowest order transition matrix elements for the electromagnetic and weak interaction $\left|M_\gamma^2 + M_Z^2\right|$. Since the weak interaction is parity violating, M_Z takes different values for the two helicity states, so that one has slightly different detector rates R^+ and R^-.

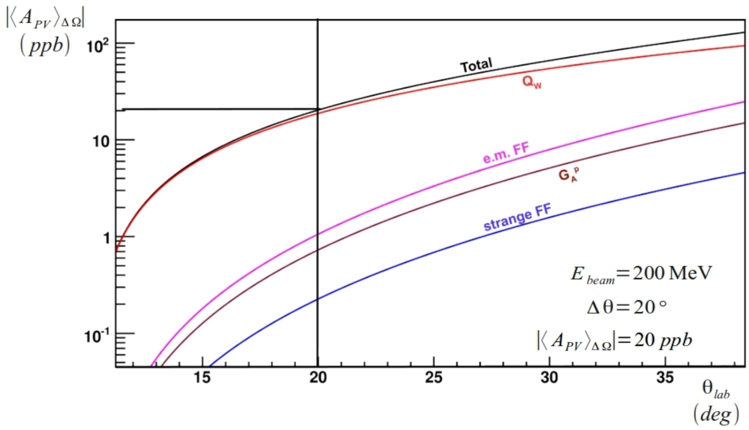

Fig. 4 Parity violating asymmetry, averaged over detector acceptance, vs. laboratory scattering angle θ_{lab}. The calculation has been done for 200 MeV beam energy and a polar acceptance of $\Delta\theta = 20°$. Shown is the running of the total asymmetry as well as contributions from the proton form factors. The P2 collaboration is currently planning to measure at $\theta_{lab} = 20° \pm 10°$. At this angle, the total asymmetry, which is of the order of 10^{-8}, is dominated by the contribution of the proton's weak charge.

where N is the number of elastically scattered electrons, both detector acceptance and luminosity have to be huge so that high counting statistics outweight the smallness of the observable effect.

3 Achievable precision within P2

In order to estimate the achievable precision in the determination of the proton's weak charge, Monte Carlo studies have been undertaken. Within these, experimental and theory parameters have been sampled within their projected uncertainties in order to minimize the total uncertainty of $\sin^2(\theta_W)$. Fig. 5 shows an example. The results of the Monte Carlo analysis are summarized in Tab. 1.

According to the studies' results, we expect an achievable relative uncertainty of the proton's weak charge of

$$\frac{\Delta Q_W^p}{Q_W^p} = 1.9\%, \tag{5}$$

which corresponds to a relative uncertainty of $\sin^2(\theta_W)$ of

$$\frac{\Delta\left(\sin^2\theta_W\right)}{\sin^2\theta_W} = 0.15\%. \tag{6}$$

The analysis of A_{PV}-measurements with the aim to extract the weak charge

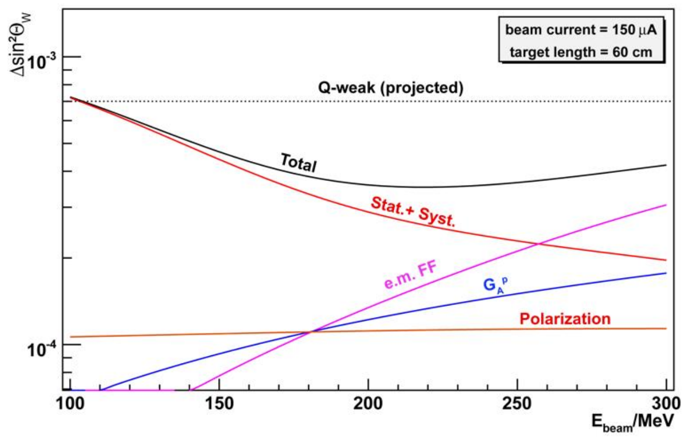

Fig. 5 Uncertainty of $\sin^2(\theta_W)$ vs. beam energy. The calculations assume a beam current of 150 μA, a 60 cm long liquid-hydrogen target, a beam polarization $P = 85\% \pm 0.5\%$, $\theta_{lab} = 20° \pm 10°$, full azimuthal coverage and 10000 hours of measurement time. The plot shows the expected total uncertainty of $\sin^2(\theta_W)$ (black), contributions from nuclear form factors as well as contributions from statistical and systematical uncertainties.

Table 1 Parameters and results of the Monte Carlo study

Beam energy	200 MeV
Beam current	150 μA
Polarization	(85±0.5)%
Target	60 cm liquid-hydrogen
Time	10000 h
θ_{lab}	$20° \pm 10°$
$\Delta\phi_{lab}$	2π
Q^2	0.0048 GeV^2
A_{PV}	-20.25 ppb
ΔA_{PV}	0.34 ppb (0.25 ppb stat., 0.19 ppb syst., 0.17 % rel.)
$\Delta \sin^2(\theta_W)_{tot}$	$3.6 \cdot 10^{-4}$ ($2.8 \cdot 10^{-4}$ stat., 0.15 % rel.)
$\Delta Q_W(p)$	$1.44 \cdot 10^{-3}$ (1.9 % rel.)

of the proton demands full control over higher-order corrections to Q_W^p and other parity-violating contributions. A great advantage of measuring at beam energies around 200 MeV is that the contributions from γ-Z box diagrams are under much better control compared to the case of higher beam energies ([6] and [7]). Generally, the contribution's uncertainties rapidly grow with increasing Q^2 values, as is shown in figure 6. In order to support P2 data analysis, a careful re-validation of higher-order corrections to Q_W^p will be performed in Mainz.

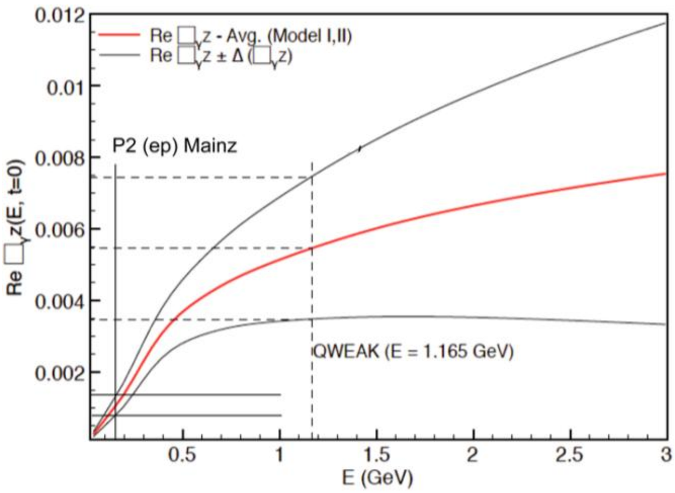

Fig. 6 Higher-order corrections to Q_W^p from γ-Z box diagrams, taken from [6]. The uncertainty of the correction rapidly grows with increasing beam energy. The resulting uncertainties for the QWeak Experiment [3] and the new P2 experiment are indicated.

4 Concept studies for the P2 experiment

In order to achieve the precision predicted by the Monte Carlo studies (section 3), on the accelerator side, we are facing very tight specifications with respect to beam parameter stability. Fortunately, with the new MESA accelerator [5] being granted in the course of the German Excellence Initiative in July 2012, a suitable machine is now being planned and will be constructed in Mainz. MESA will be independent of the currently existing MAMI accelerator and provide approximately 4000 h of beamtime per year for the P2 experiment, which will allow for a quick completion of the envisaged initial measurement program in about two to three years.

Demanding is also the projected uncertainty of 0.5 % for the polarization measurement. To reach this very high precision, a hydro-Møller-polarimeter will be used. It will consist of a target of hydrogen atoms trapped in a 8 T solenoidal magnetic field with complete electron-spin polarization. With such a non-invasive polarimeter, a sufficient statistical accuracy can be achieved within half an hour at experimental conditions.

Due to the need for a high luminosity and large detector acceptance in order to quickly gain high counting statistics, it is necessary to have a very good background suppression. At full beam current the total electron rate yielding from elastic e-p-scattering is 0.44 THz, which means that an integrating measurement is going to be necessary. Fig. 7 shows a possible detector setup, in which a solenoidal magnetic field of approximately 1 T is used to seperate electrons from elastic e-p-scattering from charged background.

Currently, concept studies with ROOT and Geant4 are being done to find the best possible detector and field configuration. Fig. 8 shows projections of

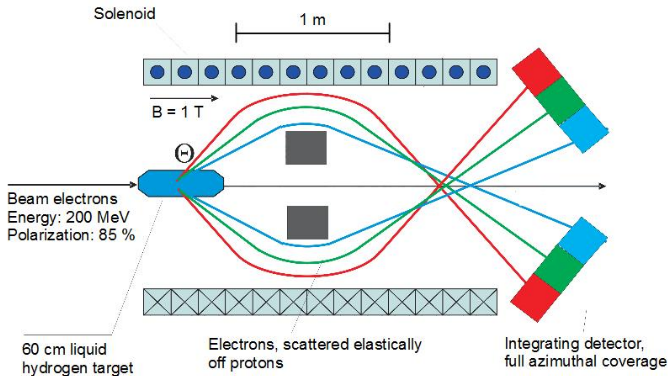

Fig. 7 Possible detector concept for P2: Beam-electrons are scattered off protons in a 60 cm long liquid-hydrogen target. They are then separated from charged background in the magnetic field of a solenoid and finally detected in an integrating detector, which covers the full azimuth. Shielding of Bremsstrahlung will be required.

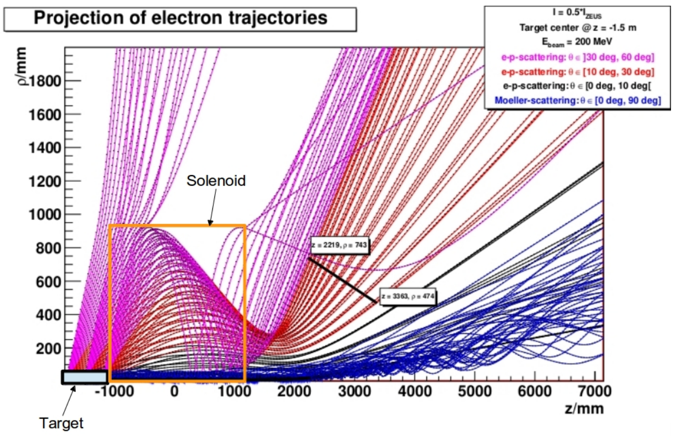

Fig. 8 Tracking of scattered electrons in the magnetic field of a solenoid with ROOT and Geant4: The beam direction is along the z-axis, ρ is the distance to the beam axis. The maximum field strength along the beam axis is 0.9 T. The beam electrons with an energy of 200 MeV are scattered in the target volume (light blue rectangle) and take spiral trajectories in the magnetic field of the solenoid (orange rectangle). Included are electrons from elastic e-p-scattering (black: $\theta < 10°$, red: $\theta \in [10°, 30°]$, pink: $\theta > 30°$) as well as Møller-scattered electons (blue: $\theta \in [0°, 90°]$). After passing the solenoid, there is a good spatial separation of the electrons scattered elastically off protons from Møller-scattered electons. The black line indicates a possible position for the integrating detector.

electron trajectories in the magnetic field of a solenoid.
In addition to concept studies with a solenoid, we are investigating on the usability of a toroidal field-setup, as it is used for example by the QWeak collaboration.

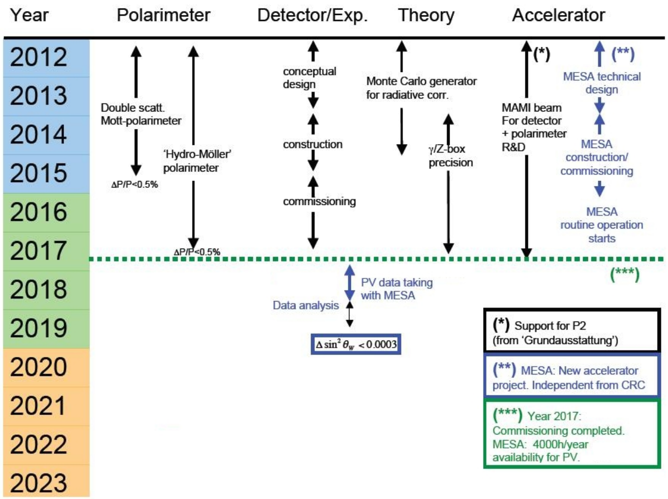

Fig. 9 Timeline of project P2 as explained in the text.

5 Timeline of project P2

P2's timeline is divided into three phases. Fig. 9 shows a schematic sketch. The first phase is devoted to preparatory work. Here the design and construction of the detector setup, the development of the high-precision polarimeters as well as the accelerator design are going to be completed. The theoretical work necessary to interpret the data will also be carried out during this phase of the project.
Phases two and three will be devoted to data taking and analysis.

References

1. J. Beringer et al. (Particle Data Group), Phys. Rev. D86, 010001 (2012)
2. D. S. Armstrong et al., JLAB-PHY-12-1478 (2012)
3. K.S. Kumar, Int. J. Mod. Phys. E19 (2010) 927-937
4. J. Erler, A. Kurylov and M. J. Ramsey-Musolf, Phys. Rev. D68, 016006 (2003)
5. R. Heine, K. Aulenbacher and R. Eichhorn, Conf. Proc. C1205201 (2012), 1993-1995
6. M. Gorchtein, C. J. Horowitz and M. J. Ramsey-Musolf, Phys. Rev. C84, 015502 (2011)
7. A. Sibirtsev, P.G. Blunden, W. Melnitchouk and A. W. Thomas, arXiv:1002.0740 [hep-ph] (2010)